Articles

Processing of Nanometer-Scale CeO_2 Particles

X.-D. Zhou,* W. Huebner, and H. U. Anderson

Electronic Materials Applied Research Center, Department of Ceramic Engineering, University of Missouri—Rolla, Rolla, Missouri 65409

Received May 23, 2002. Revised Manuscript Received September 11, 2002

A semi-batch reactor method was developed for directly synthesizing undoped and doped nanometer-scale CeO_2 particles at room temperature. Powders exhibited a surface area of ≈170 m^2/g. Control over the particle size, size distribution, and state of agglomeration could be achieved through variation of the mixing conditions and oxidation pathway.

Introduction

Over the last two decades cerium dioxide (CeO_2)-based materials have been extensively studied and employed in various applications including fast ion conductors, oxygen storage capacitors, catalysts, UV blockers, and polishing materials. Nanocrystalline CeO_2-based materials benefit not only those applications, but they also possess some other unique properties, such as the Raman-allowed modes shifting and broadening;[1] lattice expansion;[2] transition from boundary diffusion to lattice diffusion;[3] and blue shift in ultraviolet absorption spectra.[4] Doping CeO_2 with lanthanide elements (e.g., Gd^{3+}) results in the formation of oxygen vacancies, and a high ionic conductivity, σ_i. In particular, $Ce_{0.90}Gd_{0.10}O_{1.95}$ exhibits a $\sigma_i = 0.025$ $(\Omega \cdot cm)^{-1}$ at 600 °C, which is more than five times that of Y doped ZrO_2.[5] As such, $Ce_{0.90}Gd_{0.10}O_{1.95}$ is an attractive choice for use as a low-temperature electrolyte and electrode component in solid oxide fuel cells (SOFC). CeO_2-ZrO_2 solid solutions exhibit a high oxygen storage capacity (OSC) due to the high mobility of lattice oxygen in the fluorite structure. Values of OSC ≈ 6 μmol CO per m^2 have been reported.[6] The high OSC in conjunction with special redox properties (involving lattice oxygen/oxygen vacancy participation) can catalyze CO oxidation on the CeO_2 surface, making this system particularly useful in three-way catalysts for the treatment of automotive exhaust gas.[6,7]

The use of high-surface-area nanocrystalline CeO_2 powder could benefit all of these applications. This is particularly true for processing dense components, as the high melting point (2400 °C) of pure CeO_2 makes it difficult to sinter. Liquid-phase approaches that have been developed to form nanocrystalline CeO_2 powders include calcination of organic precursors, precipitation, and hydrothermal synthesis. Precursors such as oxalate,[8] ammonium carbonate,[9] and glycine/nitrate[10] have all been used, although relatively large particle sizes (≈50−100 nm) result because of the calcination process needed to decompose the organics. Precise control over the temperature is also difficult because of the exothermic pyrolysis reaction, which can lead to larger particle sizes as well as hard aggregates. Finer CeO_2 (≈10−50 nm) has been produced using ammonium hydroxide[11,12] and urea and hexamethylenetetramine.[12] However, powder agglomeration is still a problem for all of these methods.

Hydrothermal approaches to prepare CeO_2 yield powders with promising characteristics, including a fine size (∼20 nm), a narrow size distribution, single-crystal particles, high purity, and good chemical homogeneity. Greenblatt et al.[13−15] have applied this method to synthesize a series of CeO_2 solid solutions including $Ce_xLn_{1-x}O_{2-\delta}$ (Ln = La, Sm, Ca, Eu, Tb, and Pr). Hirano et al.[16] used $Ce(SO_4)_2 \cdot 4H_2O$ and ammonium hydroxide

* To whom correspondence should be addressed. Tel: 1-573-341-6131. Fax: 1-573-341-6934. E-mail: Zhou@umr.edu.

(1) Weber, W. H.; Hass, K. C.; McBride, J. R. *Phys. Rev. B* **1993**, *50*, 13297.
(2) Zhou, X.-D.; Huebner, W. *Appl. Phys. Lett.* **2001**, *79*, 3512.
(3) Zhou, X.-D.; Huebner, W.; Anderson, H. U. *Appl. Phys. Lett.* **2002**, *80*, 3814.
(4) Tsunekawa, S.; Fukuda, T.; Kasuya, A. *J. Appl. Phys.* **2000**, *87*, 1318.
(5) Steele, B. C. H. *Solid State Ionics* **2000**, *129*, 95.
(6) Deleitenburg, C.; Trovarelli, A.; Zamar, F.; Maschio, S.; Dolcetti, G.; Llorca, J. *J. Chem. Soc., Chem. Commun.* **1995**, *21*, 2181.
(7) Shelef M.; Graham, G. W. *Catal. Rev.* **1994**, *36*, 433.
(8) Van Herle, J.; Horita, T.; Kawada, T.; Sakai, N.; Yokokawa H.; Dokiya, M. *J. Am. Ceram. Soc.* **1997**, *80* (4), 933.
(9) Liu W.; Stephanopoulos, M. F. *J. Catalyst* **1995**, *153*, 304.
(10) Marina, O. A.; Bagger, C.; Primdahl S.; Mogensen, M. *Solid State Ionics* **1999**, *123*, 199.
(11) Lin J.-D.; Duh, J. G. *J. Am. Ceram. Soc.* **1997**, *80* (1), 92.
(12) Chen, P. L.; Chen, I. W. *J. Am. Ceram. Soc.* **1993**, *76* (6), 1577.
(13) Huang, W. S.; Shuk P.; Greenblatt, M. *J. Electrochem. Soc.* **2000**, *147* (2), 439.
(14) Shuk, P.; Greenblatt, M.; Croft, M. *Chem. Mater.* **1999**, *11* (2), 473−479 .
(15) Yamashita, K.; Ramanujachary, K. V.; Greenblatt, M. *Solid State Ionics* **1995**, *81* (1−2), 53−60 .
(16) Hirano, M.; Kato, E. *J. Mater. Sci. Lett.* **1996**, *15*, 1249.

10.1021/cm020597c CCC: $25.00
Published on Web 12/24/2002

as the precipitant, and was able to achieve crystallite sizes between 3 and 9 nm depending on the treatment temperature and time.

In this research, a semi-batch reactor was used to synthesize nanometer CeO_2 particles. Semi-batch reactors are widely used in the chemical industry as both laboratory equipment and in production plants to study the effects of micromixing and macromixing on the precipitate particle size distribution (PSD).[17] Typically, semi-batch reactors yield micron or submicron powders; the intent of this work was to produce finer particles through characterizing and controlling the nucleation and growth mechanisms.

Experimental Procedure

Semi-batch reactor synthesis of powders is a precipitation process, but with control over the nucleation and growth mechanisms achieved by high-speed mixing with an impeller. In this case a cerium nitrate hexahydrate, $Ce(NO_3)_3{\cdot}6H_2O$, (GIF, 99.9%) solution (0.6 to 0.8 $\times$ 10^{-3}mol/g) was added at a rate of 5 mL/min to an aqueous ammonium hydroxide precipitant (1.2−1.5 $\times$ 10^{-3}mol/g). Nitrates of Sm, La, or Gd were used as the dopant precursor. Oxygen was bubbled into the reactor with passage through a gas distributor to oxidize the Ce^{3+} to Ce^{4+}. Excessive precipitant was used so that the pH value was $\approx$ 9 after the reaction was complete. Precipitates were vacuum-filtered into a cake, washed with water and ethanol, and then vacuum-dried in air at room temperature. Whereas the initial precipitates are $Ce(OH)_3$, the oxidation and drying steps directly yield CeO_2 particles.

The particle size and morphology were determined by transmission electron microscopy (TEM, Philips EM420). Samples for the TEM were prepared by ultrasonically dispersing the powders in ethanol, and then droplets were placed on carbon-coated Cu grids. Corresponding electron diffraction patterns (EDF) were used to characterize the particle crystallinity, as well as X-ray diffractometry (XRD; Scintag 2000). The specific surface areas (SSA; m^2/g) of powders were measured by the Brunauer−Emmett−Teller (BET) method (Quantachrome; Nova 1000). From the SSA data, the particle size (d_{BET}, μm) was calculated by $d_{BET} = 6/(\rho SSA)$, where ρ is the density of the powders (g/cm^3). The theoretical density of CeO_2 was calculated using the lattice parameters calculated from the XRD pattern. X-ray line broadening ($20° \le 2\theta \le 100°$) was used to calculate the X-ray coherence length, which corresponds to the particle size after correcting for strain effects using the Lorentz intensity breadth. The theoretical densities, ρ_{th}, (kg/m^3) of the lanthanide-doped CeO_2 (Ln = La, Sm, and Gd) compositions were calculated using

$$\rho_{th} = \left(\frac{4}{n_A a^3}\right)[M_{Ce}(1 - x) + M_{Ln}x + M_O(2 - 0.5x)], \quad (1)$$

where M_{Ce}, M_{Ln}, and M_O are the molecular weights of the subspecies in kg/mole, n_A is Avogadro's number (6.023 $\times$ 10^{23}/mole), and a(m) is the XRD lattice parameter. All lanthanide elements were assumed to be in the 3+ valence state.[18]

Results and Discussion

The liquid-phase precipitation process includes three steps: chemical reaction, nucleation, and crystal growth. In most cases these three steps are fast ($\le \mu$sec), hence the mixing step has a large influence on the product particle size and its distribution. This effect has been analyzed in detail[19] and has been named either macromixing, mesomixing, or micromixing depending upon the scale level at which control is exercised. Figure 1 is a schematic diagram that illustrates these scale levels. Macromixing concerns the fluid transport step, in which the feeding droplet is divided into fluid elements on the Kolmogoroff length scale. This is the minimum size that turbulent flow can achieve. The onset of turbulent flow occurs when the Reynolds number, R_e, is $\ge 1{\cdot}10^4$. The Reynolds number is defined by $R_e = D^2N\rho/\mu$, where D is the impeller diameter (m), N is the impeller speed (rpm), ρ is the liquid density (kg/m^3), and μ is the liquid viscosity (cp). Once the fluid elements are in the Kolmogoroff length scale, micromixing takes place by molecular diffusion. This ultimately controls the supersaturation level, and importantly the local concentration of reactants. Fast reactions are often localized to the region near the feed point, where the so-called mesomixing might be slower than micromixing. [20]

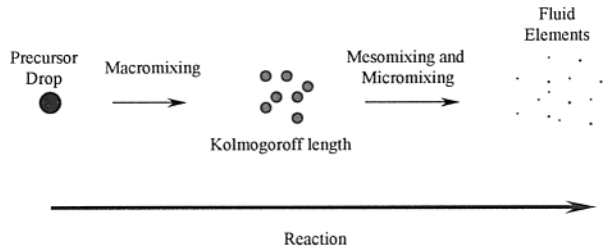

Figure 1. Schematic of the scale of the mixing steps.

Influence of Impeller Speed. Initial experiments focused on the influence of the impeller speed on the particle characteristics. Two impeller speeds were used, 100 and 500 rpm, corresponding to a $R_e \approx 2.6{\cdot}10^3$ and $1.3{\cdot}10^4$, respectively. Figure 2 a and b show the TEM micrographs of the resultant CeO_2 particles. At the low impeller speed, the particles were highly agglomerated, with a primary particle size of 5−10 nm. At 100 rpm, the fluid in the reactor is in the laminar flow state; in this case the chemical reaction takes place in the macromixing region (Figure 1). Hence, even though nanocrystalline $Ce(OH)_3$ formed at the droplet surface, this formation reaction was accompanied by agglomeration. Increasing the impeller speed to turbulent conditions did not change the primary particle size, but did significantly decrease the agglomerate size. The precipitation reaction took place in the short diffusion range (less than Kolmogorov length), in which micromixing controlled the nucleus formation and agglomeration. All pursuant studies were performed under turbulent conditions.

Influence of Feeding Method. Certainly the nucleation and growth of the $Ce(OH)_3$ occurs at the droplet−reactant interface, which opens up the possibility for processing options. In the previous section the cerium salt was introduced into the precipitant as a droplet (SIP: salt into precipitant). The cerium salt can also initially be in the reactor, with droplets of ammonium hydroxide solution added as a droplet (PIS: precipitant into salt). The difference between the two methods will be the pH value at which crystallization takes place.

(17) Nauman, E. B. *Chemical Reactor Design*; Wiley: New York, 1987.
(18) Bailar, J. C., Jr., Emeléus, H. J., Trotman-Dickenson, A. F., Eds. *Comprehensive Inorganic Chemistry*; Pergamon Press: New York, 1973.
(19) Baldyga, J.; Bourne, J. R. *Chem. Eng. Commun.* **1984**, *28*, 231.
(20) Baldyga, J.; Bourne J. R.; Hearn, S. J. *Chem. Eng. Sci.* **1997**, *52* (4), 457.

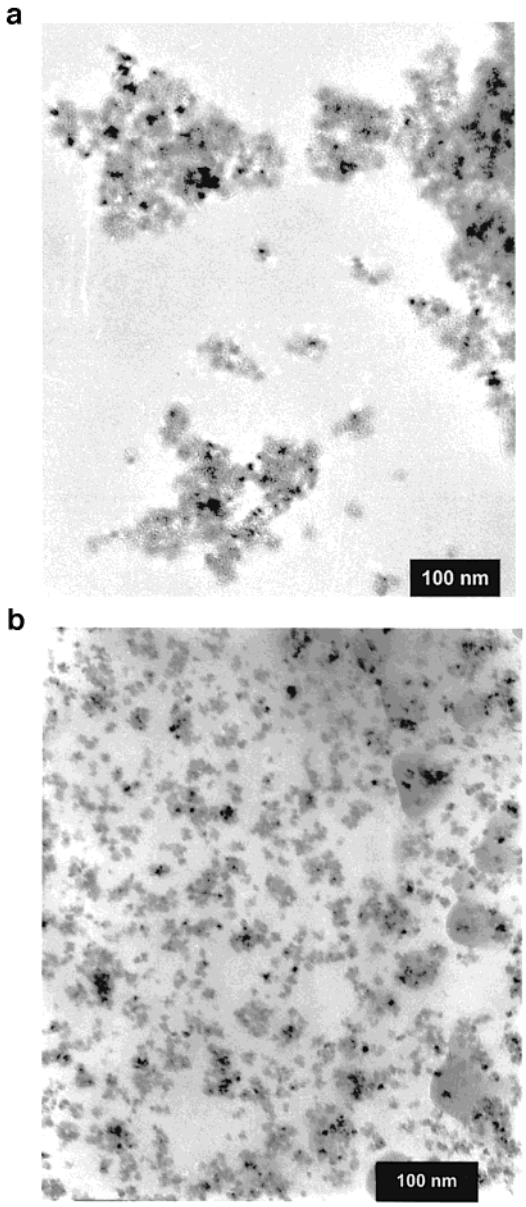

Figure 2. TEM images of the powders prepared at (a) low stirrer rate (SIP, oxygen), and (b) high stirrer rate (SIP, oxygen).

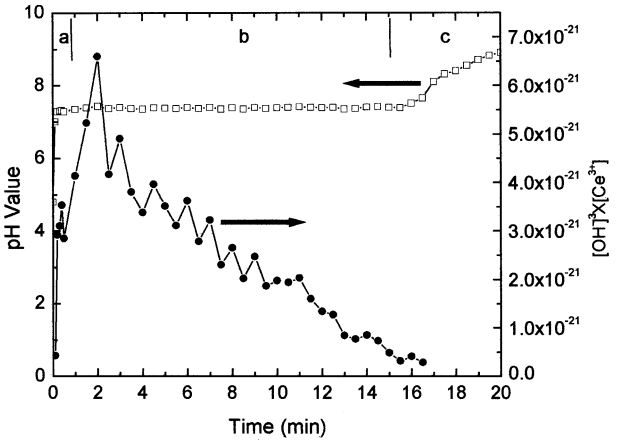

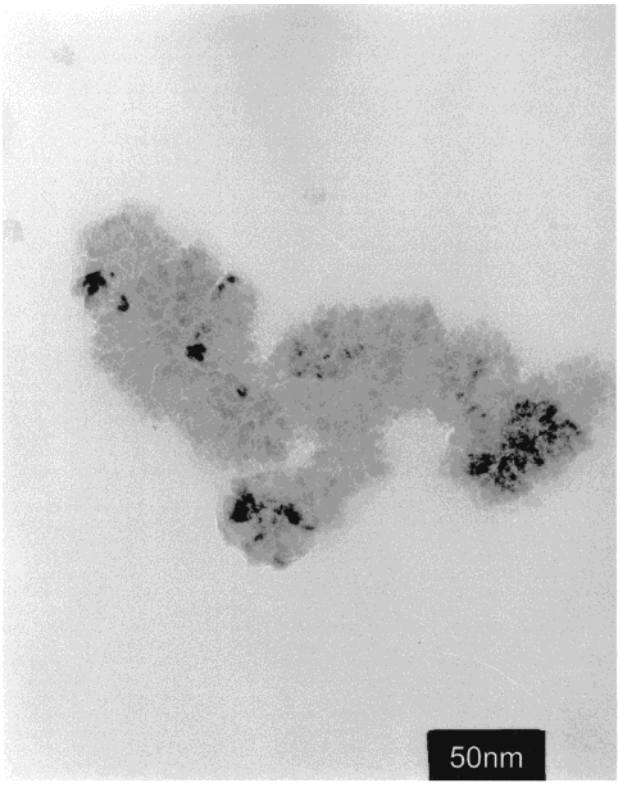

Figure 3. (a) pH Evolution and the cerium ion dissipation in PIS process (N = 500 rpm, without oxygen) Color: a, purple; b, brown; c, dark brown. (b) TEM image of the powders prepared from PIS process (N = 500 rpm, without oxygen.).

Both processes were studied in order to determine their influence on the particle characteristics.

In the case of PIS, the pH value in the reactor was initially very low (pH ≈ 3.8−4.3 for the cerium nitrate solution), and increased rapidly with just a few drops of ammonium hydroxide to a value of ∼7.2 (Figure 3 a). Further additions resulted in a slight but steady increase in pH as the Ce^{3+} ions were consumed, with a sharp transition of pH value when the reaction was close to the end. The solubility product, $[Ce^{3+}][OH^-]^3$, is also shown in Figure 3 a. This value is less than the critical solubility constant of $Ce(OH)_3$, which is ≈ $7 \cdot 10^{-21}$. Under these conditions then, even though a nucleus may form at the interface, it is in an unstable state because of the low pH value of the bulk solution. The redissolution process is called ripening. Figure 3 b is a TEM image of the product formed from the PIS process. Although the primary particle size is ∼10 nm, the agglomerates are large and nonuniform in shape. Chen et al.[12] observed similar behavior when adding ammonium hydroxide to cerium nitrate. Interesting changes in the color of the solution occurred during this process (labeled in Figure 3 a). Initially the slurry was purple (low pH), transitioned to brown (intermediate pH), and then turned yellow (high pH). These color changes are undoubtedly related to the valence state of the Ce; most likely purple corresponds to Ce^{3+} and yellow corresponds to Ce^{4+}. Further UV−Vis studies would be necessary to answer this question more completely.

Figure 4 a shows the pH value evolution during the SIP process; the pH value always remained higher than 9 (i.e., $[OH^-]$ higher than 10^{-5}mol/L). Under these basic conditions, the solubility product is much higher than the solubility constant, meaning the supersaturation value, $S = {}^{[Ce^{3+}][OH^-]^3}/_{K_{sp}}$, is very large. This results in homogeneous nucleation;[3] Figure 4 b is a TEM image

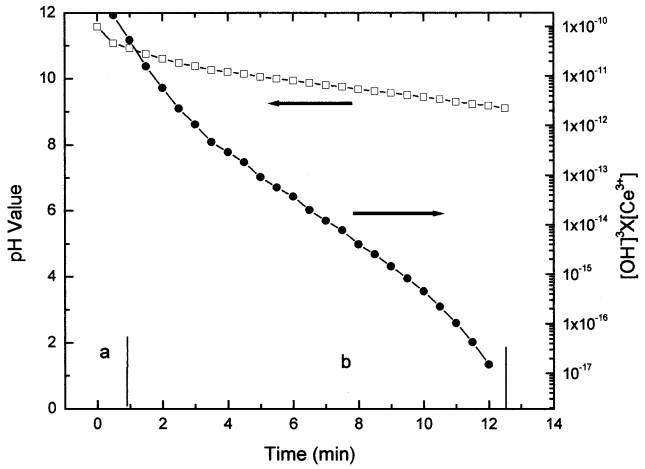

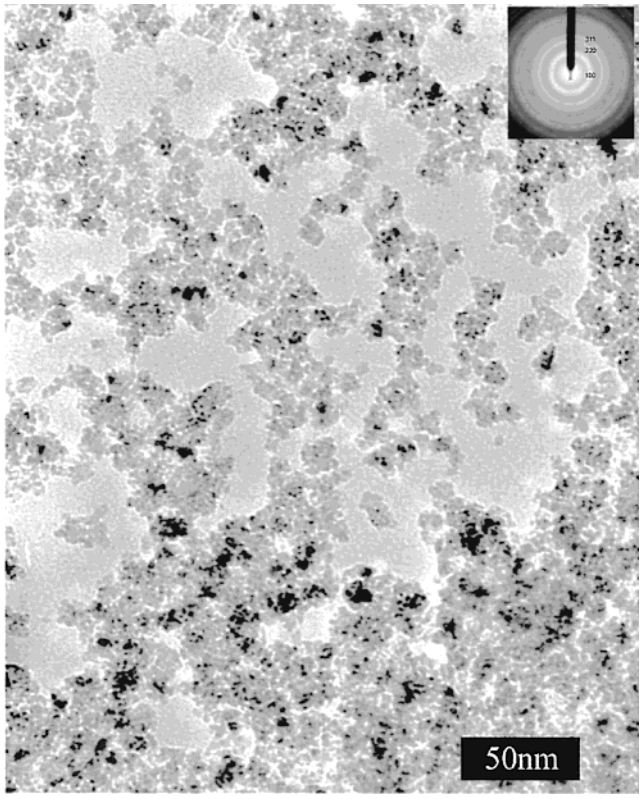

Figure 4. (a) pH Evolution and the precipitant dissipation in SIP process (N = 500 rpm, without oxygen) Color: a, brown; b, light yellow. (b) TEM image of the powders prepared from SIP process (N = 500 rpm, without oxygen.

of these particles. The primary particle size is again ~10 nm.

Some question remains concerning the reaction pathway that results in the precipitation of the $Ce(OH)_3$. That is, do they form directly from the Ce^{3+} in solution, or from an intermediate solution species, $Ce(OH)^{3+}$ (ref 12). From an electrochemical reaction point of view, the formation of $Ce(OH)^{3+}$ follows the reaction

$$Ce^{3+} + H_2O \leftrightarrow Ce(OH)^{3+} + H^+ + e', \; E° = -1.715 \text{ eV}, \quad (2)$$

where $E°$ is the standard emf value.[21] For a $[H^+] \leq 10^{-10}$ mol/L, the emf calculates to be −1.1 eV, meaning that this reaction is unfavorable.

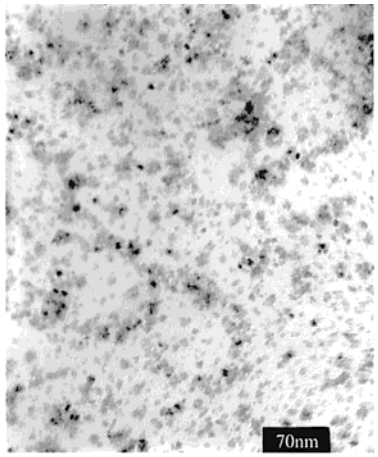

Figure 5. TEM image of the particles from the process with oxygen (N = 500rpm, SIP).

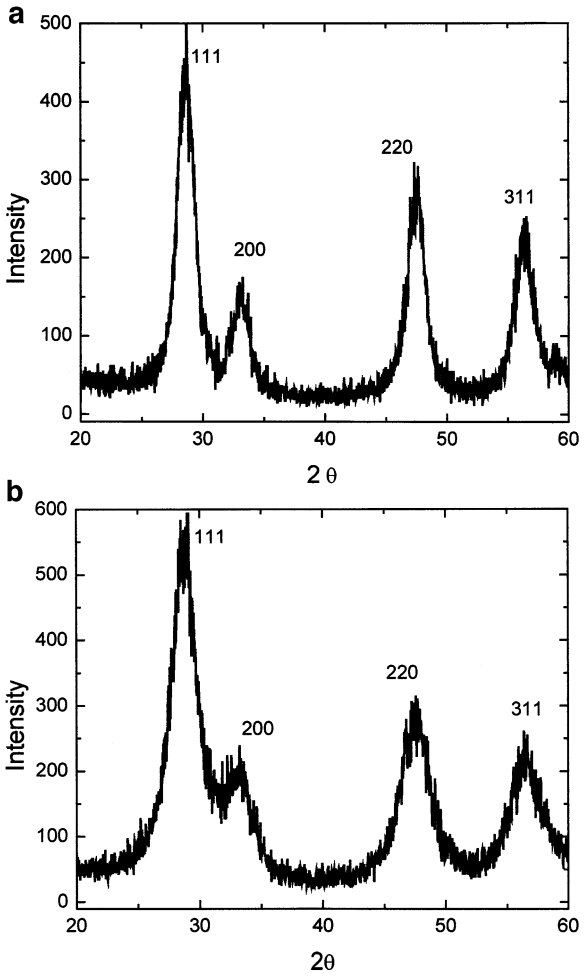

Figure 6. (a) XRD pattern of the particles from the process without oxygen (N = 500 rpm, SIP) Crystal size is 5 nm from XRD line broadening analysis. (b) XRD pattern of the particles from the process without oxygen (N = 500rpm, SIP) Crystal size is 3 nm from XRD line broadening analysis.

Influence of Oxygen Bubbling. Precipitates of $Ce(OH)_3$ transform to CeO_2 during the drying step according to the following reaction

$$2\ Ce(OH)_3 + {}^1/_2\ O_2 \rightarrow 2\ CeO_2 + 3\ H_2O \quad (3)$$

For instance, a powder cake after filtration appears brown due to the presence of $Ce(OH)_3$ (purple) and CeO_2

(light yellow), but with aging under ambient conditions transforms to a totally light yellow powder (CeO_2). Drying under a vacuum can accelerate this process; large amounts of water condense on the container walls as H_2O is released according to eq 3.

These observations led to the exploration of bubbling O_2 in the batch reactor during the SIP process to see if any changes in the particle size, morphology, or composition would occur. Initially the ammonium hydroxide was bubbled for 1 min, and then the SIP process was engaged. Droplets of the $Ce(NO_3)_3 \cdot 6H_2O$ solution added to the ammonium hydroxide caused the entire slurry to immediately turn purple, but then over a period of ~30 s would transition through a dark brown to light yellow color. Certainly the light yellow color is due to the presence of CeO_2. The purple or brown color depends on the relative concentration of compounds containing Ce^{3+} or Ce^{4+}. Similar results were found by Fahrenholtz[22] who observed color changes in a $Ce(OH)_3$ suspension with aging (up to 48 h) in a beaker. In this case the dissolved O_2 most likely caused the slow color changes.

Figures 4 b and 5 are TEM images of the CeO_2 prepared without and with O_2. These figures reveal that the O_2 results in a finer particle size and powders that are less agglomerated. Evidently when the decomposition reaction proceeds in air, the powders tend to be more strongly agglomerated. That said, these powders are still lightly agglomerated, as they can be redispersed in a solution. Figure 6 a and b are the corresponding XRD patterns. Line broadening analysis indicates the O_2 decreased the primary particle size to 3 nm, compared to 5 nm without O_2.

Understanding why the primary particle size changes is not simple to address. The overall results indicate that the nucleation step is the fastest, meaning that $Ce(OH)_3$ formation is immediate, and would not be impacted by the presence of an O_2 bubble. The oxidation reaction of $Ce(OH)_3$ (equation 3) can take place either at a gas−solid interface (i.e., at the surface of the bubble), or with dissolved O_2. An O_2 flow rate of 5 cm^3/sec, with a bubble size of 1 mm [23] corresponds to an increase in the effective surface area of only from 50 cm^2 (reactor cross area) to 87 cm^2. Whether this is sufficient to significantly affect the kinetics is undetermined. Perhaps the greater effect is one in which the bubbling O_2 simply maintains an equilibrium concentration of dissolved O_2 as it is consumed. The equilibrium concentration of O_2 in water−ammonium hydroxide solutions ranges from 10 to 25 ppm.[24] With the liquid volume of a 500-mL batch reactor this would be an order of five insufficient to fully oxidize a typical batch size (~10 g) of $Ce(OH)_3$. In any case, the use of O_2 bubbling during the SIP process yields the finest, least agglomerated, CeO_2 powder.

Summary and Conclusions

In this work a new process, the semi-batch reactor, was developed for synthesizing nanometer-scale CeO_2 particles. This process directly yields single-crystal, 3−5 nm particles at room temperature. The corresponding surface area was ~170 m^2/g. The precursor mixing technique was the most significant factor for controlling the particle size, size distribution, and state of agglomeration. Feeding the cation solution into the precipitant, the SIP process, resulted in the finest size and least agglomeration. In addition, introducing oxygen into the batch reactor was found to decrease the agglomerate and particle size.

CM020597C

(21) Lide, D. R. *CRC Handbook of Chemistry and Physics*, 76th ed.; CRC Press: Boca Raton, FL, 1996.
(22) Fahrenholtz, W. Personal communication.
(23) Barigou, M.; Greaves, M. *Chem. Eng. Sci.* **1992**, *47*, 2009.
(24) Battino, R. *Oxygen and Ozone*; Pergamon Press: New York, 1981.